

3.1 THUNDERSTORM ELECTRICAL STRUCTURES OBSERVED BY LIGHTNING MAPPING ARRAYS

Kyle C. Wiens*

Los Alamos National Laboratory, Los Alamos, New Mexico

1. INTRODUCTION

Lightning mapping arrays (LMAs: Rison et al., 1999; Krehbiel et al., 2000; Hamlin, 2004) use Global Positioning System time of arrival to locate very high frequency radiation sources emitted by lightning discharges. For a given lightning flash, an LMA may locate thousands of such sources which provides detailed maps of the total lightning activity and allows for diagnosis of the time-evolving three-dimensional charge structure of thunderstorms.

This paper first provides a very brief introduction to LMAs, followed by a description of how LMAs have been used to determine the qualitative charge structure of thunderstorms. Some examples of thunderstorm charge structures are then presented. Though LMAs have been operated since 1998 in several locations across the United States, the examples presented here are from storms observed during the Severe Thunderstorm Electrification and Precipitation Study (STEPS: Lang et al., 2004). The diagnosed charge structures of these storms evolved with time and ranged from normal tripole to inverted dipole to far more complex charge structures. Based on the limited number of storms analyzed thus far using the LMA charge structure methodology, it appears that the parent charge structure of a given storm determines the dominant polarity of cloud-to-ground (CG) flashes the storm produces. Storms with normal tripole charge structures produce mainly negative CG flashes, while storms with “inverted” charge structures produce mainly positive CG flashes. In both cases, the CG flashes require the presence of a lower charge region: lower positive charge in the case of normal tripole storms, and lower negative charge in the case of “inverted” storms.

2. How the LMA Works

The following is a very brief description of how LMAs work. More detailed descriptions can be found elsewhere [e.g., Rison et al., 1999; Krehbiel et al., 2000; Hamlin, 2004; Thomas et al., 2004; Wiens, 2005].

A typical LMA consists of a dozen or so antennas spaced 10s of kilometers apart. Each of the LMA antennas accurately records the time of arrival (TOA) of very high frequency (VHF) radiation emitted by impulsive accelerations of charge during lightning discharges. Each of these impulsive accelerations is termed an event or a source. The time and three-dimensional location of each source is determined by differential-time-of-arrival. For a given lightning flash, the LMA may locate hundreds to thousands of such VHF sources, resulting in detailed maps of the total lightning activity. LMAs can be used to reveal many characteristics of thunderstorms, including estimation of total (intra-cloud plus cloud-to-ground) flash rates. This paper focuses on how LMAs can be used to determine qualitative thunderstorm charge structure.

a. Charge Structure Determination

Charge structure analysis of LMA data is an interpretative process guided by a realistic physical model of the lightning discharge. Recent interferometer measurements [Rhodes et al., 1994; Shao and Krehbiel, 1996] and LMA measurements [Rison et al., 1999; Krehbiel et al., 2000; Hamlin, 2004; Thomas et al., 2004] support the bi-directional model which was originally proposed by Kasemir (1960) and recently advocated and described by Mazur and Ruhnke (1993). In this model, the lightning discharge initiates in the strong electric field between regions of net positive and negative charge. The discharge then propagates in opposite directions from the discharge origin with one direction advancing negative charge (called negative breakdown or negative leaders) and the other direction advancing positive charge (positive breakdown or positive leaders). The charge block experiments of Williams et al. (1985) and modeling studies of Mansell et al. (2002) provide circumstantial evidence that the discharges preferentially propagate into regions of higher charge density, with much denser branching in these regions.

Using this bi-directional model as a basis for physical interpretation, the temporal and spatial development of individual flashes can be examined in a time-animated sense to infer the signs and locations of the charge regions involved in the flashes. As described in Rison et al. (1999), negative polarity breakdown is inherently noisier than positive polarity breakdown at the radio frequencies used by the LMA, resulting in far more LMA sources

*Corresponding author address: Kyle C. Wiens, Los Alamos National Laboratory, ISR-2, Space and Remote Sensing Sciences Group, Los Alamos, NM 87545; email: kwiens@lanl.gov

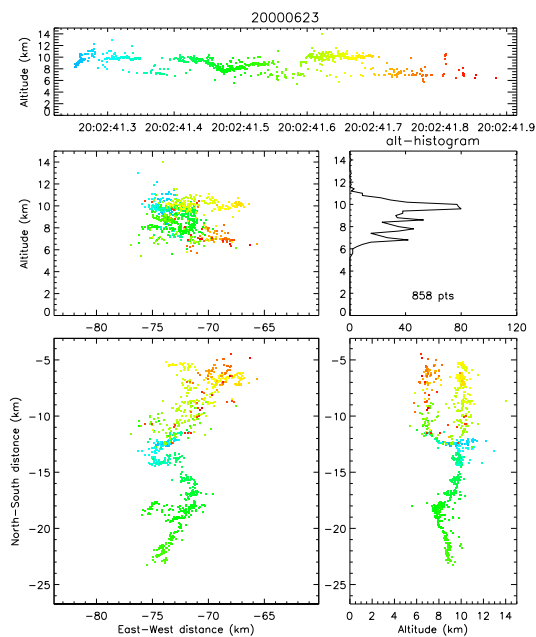


Figure 1: Lightning mapping of a single flash in a storm observed on 23 June 2000 during STEPS. The flash duration is 65 ms. Top panel shows altitude versus time. Lower panels show three different spatial projections along with an altitude histogram of the number of sources. LMA sources are color-coded by time from blue to red. This is a ‘normal’ IC flash that initiated upward from an inferred negative charge region at 6–7 km altitude into an inferred positive charge region at 8–10 km altitude. The stratification of the charge regions is most evident in the N-S vs altitude projection in the bottom-right panel. Adapted from Wiens (2005).

that map the negative breakdown than map the positive breakdown. Assuming that negative breakdown usually proceeds through positive charge regions, a given flash has a relatively greater number of LMA sources within (or indicative of) the positive charge region(s) involved in the flash. In addition, partial mapping of negative charge regions is possible when negative leaders retrace the path of the quieter positive leader. This retracing of the positive channel by negative breakdown seems to correspond to the ‘recoil streamers’ described by Mazur and Ruhnke (1993).

For a typical intra-cloud (IC) flash between two charge regions, the lightning mapping generally reveals a stratified bi-level structure. For example, Fig. 1 shows the lightning mapping of a single IC flash from the early stages of the 23 June 2000 storm observed during STEPS. Here, the relative number of LMA sources in each inferred charge region gives a rough idea of the charge structure (in the case of this flash, positive charge

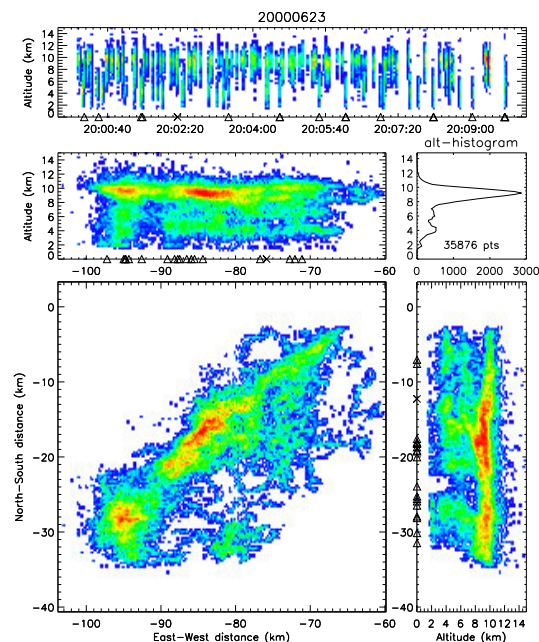


Figure 2: Ten minutes of lightning mapping from a line of storms on 23 June 2000 observed during STEPS. Layout is the same as in Fig. 1, but here the LMA sources are color-coded by source density, with warmer colors indicating greater concentration of LMA sources. Black triangles show locations of NLDN-reported –CG strikes. Adapted from Wiens (2005).

over negative charge). This structure is even more pronounced in Fig. 2 which shows 10 minutes worth of lightning mapping surrounding the flash shown in Fig. 1. In Fig. 2, the LMA sources are plotted as the number density, with warmer colors indicating a greater number of sources. The vast majority of LMA sources reside between 8 and 10 km altitude, indicating the upper-positive charge region. Secondary peaks in the altitude distribution at 6 and 4 km indicate the mid-level negative charge and lower-positive charge regions, respectively (as described below).

As illustrated in the previous paragraph, one can get a *rough* idea of the vertical charge structure based only on the altitude distribution of LMA sources; however, careful analysis of the spatial and temporal development of individual flashes is a more revealing and reliable way to identify the polarity of the charge regions involved. Since the LMA primarily detects negative breakdown, the propagation direction of the first several sources of a flash are assumed to correspond to negative breakdown that propagates in a direction opposite that of the electric field vector, i.e., the lightning mapping of each flash is assumed to initially progress toward positive charge and

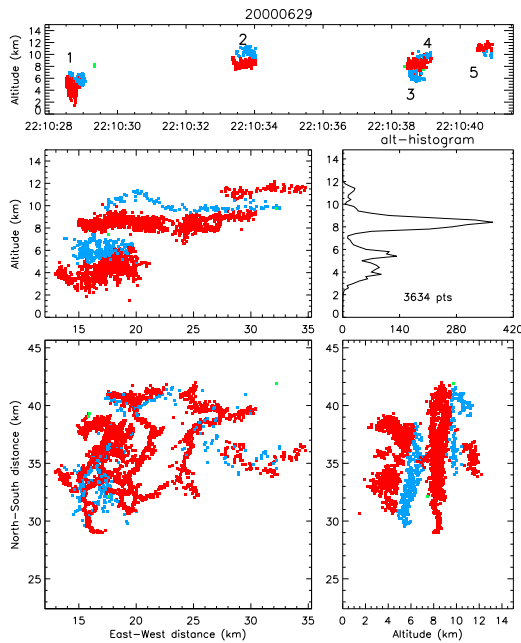


Figure 3: Lightning mapping of five intra-cloud flashes (two normal, three inverted) showing 5-layer charge structure during the early development of the 29 June 2000 supercell storm observed during STEPS. The LMA sources are color-coded by inferred ambient charge (red=positive, blue=negative, green=undetermined). Adapted from Wiens et al. (2006).

away from negative charge. Coleman et al. (2003) found very good agreement between LMA-inferred charge structure and balloon soundings of electric field. The location of LMA-inferred flash initiation agreed well with the balloon-inferred heights of maximum electric field, and the lightning preferentially branched into “wells” of electrostatic potential, which are typically coincident with regions of large net charge density. These results from Coleman et al. (2003) support the previously mentioned results from the charge block experiments of Williams et al. (1985) and the modeling studies of Mansell et al. (2002).

As a more explicit illustration of this flash-by-flash charge structure methodology, Fig. 3 shows lightning mapping of a five-flash sequence during the early stages of the 29 June 2000 supercell observed during STEPS. Here, the lightning mapping reveals five vertically stacked charge regions, alternating in polarity with positive the lowest. The sources are color-coded by inferred ambient charge region to highlight the stratified structure. Figure 4 shows the second flash of this five-flash sequence, with the sources color-coded by time. The initial negative breakdown of this flash proceeded *downward* from 9.5 km MSL then progressed through an

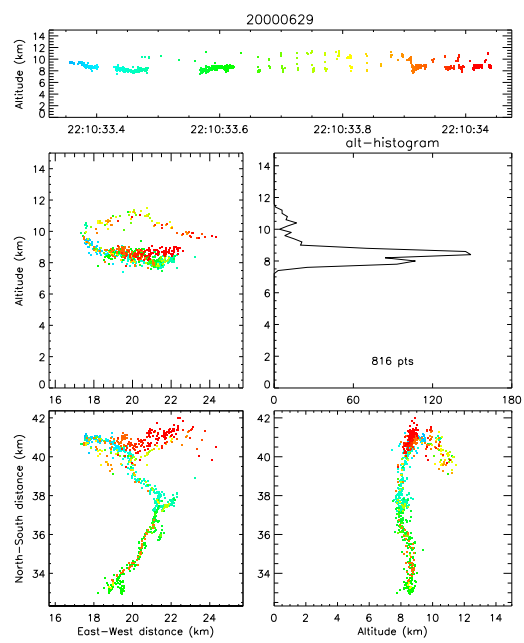


Figure 4: Lightning mapping of the second flash of the 5-flash sequence in Fig. 3. This is an “inverted” flash that initiated downward from an inferred negative charge region at 10–11 km into an inferred positive charge region at 8–9.5 km. LMA sources are color-coded by time from blue to red. Adapted from Wiens et al. (2006).

inferred stratified positive charge region at 8–9 km MSL. A distinct and more sparse grouping of sources above the initiation point mapped out the inferred negative charge at 10–11 km MSL. Additionally, some of the red-colored points late in the flash appear to have retraced the breakdown through both charge regions. Such flashes are termed “inverted” IC flashes because they reveal an inverted dipole structure. Figure 5 shows the third flash of the five-flash sequence and shares many of the features of the flash in Fig. 4, but flipped in the vertical. The initial negative breakdown of this flash progressed *upward* from 8 km MSL into the same stratified positive charge region at 8–9 km MSL that was revealed by the previous inverted flash. The sparse grouping of sources at 6–7 km MSL maps out the inferred negative charge below the positive. Such flashes are termed “normal” IC flashes as they reveal a normal dipole structure. Hence, the location of the positive charge was consistently revealed by both of these flashes. The remaining flashes of the 5-flash sequence in Fig. 3 were similarly clear, with each showing distinct bi-level structure. When put together, they reveal a very clear and consistent picture of the charge structure.

As another striking example, Fig. 6 shows the same 10-minutes of lightning mapping as Fig. 2, but here the

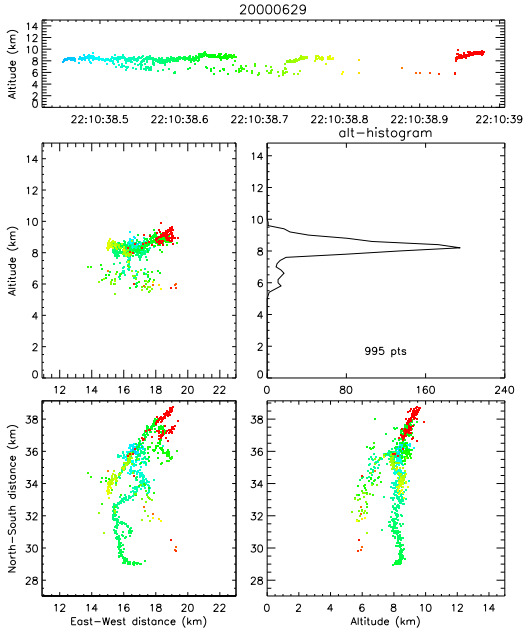


Figure 5: Lightning mapping of the third flash of the 5-flash sequence in Fig. 3. This is a “normal” flash that initiated upward from an inferred negative charge region at 6–7 km into an inferred positive charge region at 8–9.5 km. LMA sources are color-coded by time from blue to red. Adapted from Wiens et al. (2006).

inferred charge regions participating in each individual flash have been painstakingly identified, then all the flashes have been plotted as the “charge density”. This more clearly shows the vertical separation of the charge regions and illustrates how the upper-positive charge region dominates the lightning activity of this storm (at least in terms of the LMA sources).

Flash-by-flash analysis of LMA data in a time-annotated sense is certainly the best way to determine thunderstorm charge regions. However, it is a very labor-intensive process that resists automation. It is also prone to subjective interpretation and requires some degree of experience with the data. In lieu of this flash-by-flash analysis, a somewhat more objective (though not as accurate) method of determining the gross vertical charge structure is by inspection of altitude histograms of the LMA sources in comparison with altitude histograms of flash initiation heights. As mentioned above, the altitude histograms of LMA sources give a general sense of the vertical charge structure since the positive charge regions are expected to contain relatively more LMA sources. The flash initiation heights add another piece to the puzzle. These flash heights are a nice by-product of the algorithm developed by Thomas et al. (2003) which

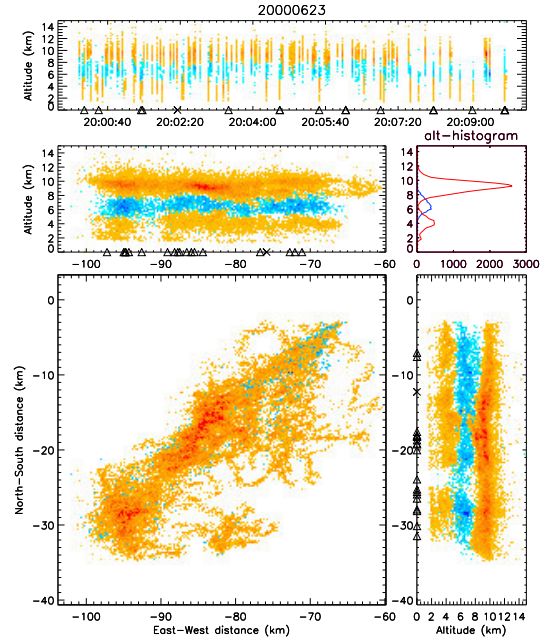


Figure 6: As in Fig. 2, but with LMA sources color-coded by inferred ambient charge density. Redder (bluer) colors indicate greater numbers of LMA sources in positive (negative) charge regions. The altitude histogram panel shows separate histograms for LMA sources in inferred positive (red) and negative (blue) charge regions. Adapted from Wiens (2005).

sorts LMA sources into discrete “flashes”. The algorithm keeps track of which sources correspond to each flash. One can then take the sources from each flash, sort them in chronological order, and determine the height at which each flash originated and in what direction it initially traveled. The origin height is just the height of the first source of the flash, and the initiation direction can be determined by regressing the altitude of the first several sources onto the time of the first several sources. If the regression coefficient is positive (negative), then the flash initiated upward (downward). If we interpret these initial flash heights and directions according to the bi-directional discharge model, then flashes that initiate upward (downward) are heading toward positive charge that lies above (below) the initiation height. Fig. 7 shows an example of these LMA histograms in comparison with vertical cross-sections of radar reflectivity and LMA source density. The LMA data used in this figure are the first 5 minutes of lightning from Figs. 2 and 6. The distributions in the LMA sources and flash start heights in Fig. 7 are generally consistent with the manual flash-by-flash charge structure determination shown in Fig. 6. The prominent upper-level peak in the LMA source altitude histogram and LMA density cross-section strongly indi-

cates the upper positive charge at 8–10 km altitude, while the smaller lower-level peak gives some indication of lower positive charge near 4–5 km altitude. As indicated by the red curve in the histogram plot of Fig. 7, most of the flashes initiated upward near 7 km, while a second distinct population of flashes initiated downward from 5 km. Hence, the upper population of upward flashes indicates the boundary between the mid-level negative charge and upper positive charge, while the lower population of downward flashes indicates the boundary between the mid-level negative charge and lower positive charge. The heights of these two flash start maxima may also be interpreted as the locations of maximum vertical electric field (e.g., Coleman et al., 2003).

3. Example storms from STEPS

The LMA used in STEPS was constructed, installed and operated by New Mexico Tech (see Hamlin, 2004; and Thomas et al., 2004). Here now are three example storms observed by the LMA during STEPS. As shown by the schematic in Fig. 10, these storms exhibited a variety of charge structures and CG lightning production:

- 23 June: A line of storms which initially had normal polarity charge structure and produced –CG flashes then switched to inverted polarity charge structure and produced +CG flashes.
- 29 June: A +CG-dominated tornadic supercell storm which, during its severe phase, had a complex charge structure that could be roughly described as an inverted tripole.
- 3 June: An isolated storm with a persistent inverted dipole charge structure that produced no CG flashes of either polarity.

Wiens (2005) provides a detailed analysis of these storms which is summarized here.

a. 23 June 2000: Switch from –CG to +CG flashes

The –CG-dominated cells in the early stages of the line of storms on 23 June 2000 followed the typical normal tripole archetype. They began with with only IC flashes between mid-level negative and upper positive charge (i.e., a normal dipole charge structure) but produced no –CG flashes (see the top-left panel of Fig. 10). As these storms developed further and precipitation grew and descended, a lower positive charge region formed within the strongest precipitation, thus completing the tripole charge structure. Negative CG flashes began only after the formation of this lower positive charge, and the –CG flashes originated between the mid-level negative and lower positive charge (see Fig. 7 and the top-middle

panel of Fig. 10). In its the later stages, convective collapse apparently led to descent of the charge regions and formation of an inverted tripole structure (see the top-right panel of Fig. 10). During this collapse, –CG flashes ceased and +CG flashes began. All of the +CG flashes originated between the mid-level positive and lower negative charge regions of the inverted tripole in the collapsing part of the storm.

b. 29 June 2000: Inverted tripole, +CG-dominated supercell

The evolution of the +CG-dominated 29 June 2000 supercell storm is illustrated schematically in the middle panel of Fig. 10 and in Fig. 9. The first 20 minutes of lightning in this storm showed only mid-level negative and lower positive charge which could be described as an inverted dipole structure. However, these two charge regions may also correspond to the two lower charge regions of a normal tripole configuration. Following a burst of updraft, additional charge regions developed above the pre-existing low inverted dipole, resulting in an overall 5-layer charge structure, alternating in polarity with positive charge nearest the ground. During the severe stage of the 29 June storm, lightning near the strong updraft revealed an elevated inverted dipole structure, while further downwind the charge was roughly an inverted tripole with negative charge nearest the ground (Fig. 8,top). This charge structure supported frequent +CG flashes and persisted for nearly three hours. The +CG flashes originated between the mid-level positive and lower negative charge on the downwind side of the precipitation core and tapped positive charge within the precipitation core and (more often) mid-level positive charge extending further downwind of the precipitation core (see, e.g., the right side of Fig. 9).

More detailed observational analysis of this storm may be found in MacGorman et al. (2005), Tessendorf et al. (2006) and Wiens et al. (2006), and a modeling study of this storm may be found in Kuhlman (2004).

c. 3 June 2000: Inverted dipole with no CG flashes

The storm on 3 June 2000 produced no CG flashes of either polarity despite frequent intra-cloud lightning. The charge structure of this storm was relatively simple (as inferred from both the LMA and an EFM balloon sounding), consisting of a vertically thin negative charge region at 10–12 km altitude, and a deep (or multi-layered) positive charge below (Fig. 8, bottom). The 3 June storm was thus structurally similar in some respects to the severe stage of the 29 June storm, but with one important difference: There was never any LMA indication of a lower negative charge region in the 3 June storm. This lack of a lower negative charge is apparently the

reason why the 3 June storm produced no +CG flashes despite its inverted charge structure.

4. Summary and Discussion

Due to the labor-intensive nature of charge structure analysis, only a handful of storms observed by the LMA have been studied. However, some tentative conclusions can be drawn from the limited set of cases described above. In the simplest vertical sense, –CG flashes resulted from a normal tripole structure, and +CG flashes result from an inverted tripole structure (e.g., Fig. 10). With little exception, +CG flashes originated between the mid-level positive and lower negative charge regions of an inverted tripole charge structure and tapped the mid-level positive charge. The –CG flashes originated between the mid-level negative and lower positive charge regions of a normal tripole charge structure and tapped the mid-level negative charge. Neither polarity of ground flash occurred without the presence of a lower charge region (lower positive charge in the case of –CG flashes, and lower negative charge in the case of +CG flashes). These vertical descriptions of the charge structure are gross simplifications, however, as the charge structure of each storm varied greatly in the horizontal and with time.

Flash-by-flash charge structure analysis of the LMA data is tedious. Though it would be difficult to accomplish, it would be a great boon if automated routines could be developed to do this. As an alternative, the altitude histograms of LMA sources and flash start heights (e.g., Figs. 7 and 8) provide a very revealing and useful way to summarize and comprehend the charge structure. Hence, in lieu of the flash-by-flash analysis, it may be more feasible to rely on such histograms (and other simple LMA plots, like source density cross-sections) to give a rough interpretation of charge structure for a larger sample of storms. However, for detailed studies, charge determination via flash-by-flash analysis should be employed.

Lightning mapping (and LMA charge determination) cannot replace in situ measurements of thunderstorm charge regions, such as those obtained from balloons and aircraft. However, it does provide a fully three-dimensional qualitative picture of the charge structure throughout the evolution of the storm to complement the quantitative information gained from in situ measurements. Furthermore, with lightning mapping, the development and evolution of charge regions can then be investigated relative to concurrent dynamical and microphysical evolution of thunderstorms.

Acknowledgments: The author thanks the LMA group from New Mexico Tech (Paul Krehbiel, Bill Rison, Ron Thomas, Tim Hamlin, Jeremiah Harlin, et al.) who provided both the LMA data and the outstanding software (XLMA) for analyzing

the data. Thanks also go to all the participants in STEPS, who are too numerous to recognize individually. The observations presented here are largely taken from the author's Ph.D. work at Colorado State University under the supervision of Steven Rutledge with funding from NSF research grants ATM-9912051 and ATM-0309303.

References

- Coleman, L. M., T. Marshall, M. Stolzenburg, T. Hamlin, P. Krehbiel, W. Rison, and R. J. Thomas, 2003: Effects of charge and electrostatic potential on lightning propagation. *J. Geophys. Res.*, **108**, doi:10.1029/2002JD002718.
- Hamlin, T., 2004: *The New Mexico Tech Lightning Mapping Array*. Ph.D. thesis, New Mexico Institute of Mining and Technology, 164 pp.
- Kasimir, H. W., 1960: A contribution to the electrostatic theory of lightning discharge. *J. Geophys. Res.*, **65**, 1873–1878.
- Krehbiel, P. R., R. J. Thomas, W. Rison, T. Hamlin, J. Harlin, and M. Davis, 2000: Lightning mapping observations in central Oklahoma. *EOS*, **81**, 22–25.
- Kuhlman, K. M., 2004: *Numerical Simulations of the 29 June 2000 STEPS Tornadoic Supercell: Microphysics, Electrification, and Lightning*. Master's thesis, Univ. of Okla., Norman, 72 pp.
- Lang, T. J., L. J. Miller, M. Weisman, S. A. Rutledge, L. J. B. III, V. N. Bringi, V. Chandrasekar, A. Dettwiler, N. Noesken, J. Helsdon, C. Knight, P. Krehbiel, W. A. Lyons, D. MacGorman, E. Rasumussen, W. Rison, W. D. Rust, and R. J. Thomas, 2004: The Severe Thunderstorm Electrification and Precipitation Study. *Bull. Amer. Meteorol. Soc.*, doi:10.1175/BAMS-85-8-1107.
- MacGorman, D. R., W. D. Rust, P. Krehbiel, E. Bruning, and K. Wiens, 2005: The electrical structure of two supercell storms during STEPS. *Mon. Wea. Rev.*, **133**, 2583–2607.
- Mansell, E. R., D. R. MacGorman, C. Ziegler, and J. M. Straka, 2002: Simulated three-dimensional branched lightning in a numerical thunderstorm model. *J. Geophys. Res.*, **107**, doi:10.1029/2000JD00244.
- Mazur, V. and L. Ruhnke, 1993: Common physical processes of natural and artificially triggered lightning. *J. Geophys. Res.*, **98**, 12 913–12 930.
- Rhodes, C. T., X. M. Shao, P. R. Krehbiel, R. J. Thomas, and C. O. Hayenga, 1994: Observations of lightning phenomena using radio interferometry. *J. Geophys. Res.*, **99**, 13,059–13,082.

- Rison, W., R. J. Thomas, P. R. Krehbiel, T. Hamlin, and J. Harlin, 1999: A GPS-based three-dimensional lightning mapping system: Initial observations in central New Mexico. *Geophys. Res. Lett.*, **26**, 3573–3576.
- Shao, X. M. and P. R. Krehbiel, 1996: The spatial and temporal development of intracloud lightning. *J. Geophys. Res.*, **101**, 26 641–26 668.
- Tessendorf, S. A., L. J. Miller, K. C. Wiens, and S. A. Rutledge, 2006: The 29 June 2000 supercell observed during STEPS. Part I: Kinematics and microphysics. *J. Atmos. Sci.*, in Review.
- Thomas, R. J., P. R. Krehbiel, W. Rison, J. Harlin, T. Hamlin, and N. Campbell, 2003: The LMA flash algorithm. *Proc. 12th Int. Conf. Atmos. Elec., Versailles, France, June 2003*.
- Thomas, R. J., P. R. Krehbiel, W. Rison, S. J. Hunyady, W. P. Winn, T. Hamlin, and J. Harlin, 2004: Accuracy of the Lightning Mapping Array. *J. Geophys. Res.*, **109**, doi:10.1029/2004JD004549.
- Wiens, K. C., 2005: *Kinematic, Microphysical, and Electrical Structure and Evolution of Thunderstorms during the Severe Thunderstorm Electrification and Precipitation Study (STEPS)*. Ph.D. thesis, Colorado State University, Fort Collins, 295 pp.
- Wiens, K. C., S. A. Rutledge, and S. A. Tessendorf, 2006: The 29 June supercell observed during STEPS. Part II: Lightning and charge structure. *J. Atmos. Sci.*, in Press.
- Williams, E. R., C. M. Cooke, and K. A. Wright, 1985: Electrical discharge propagation in and around space charge clouds. *J. Geophys. Res.*, **90**, 6059–6070.

23 June, Storm 1 (early)

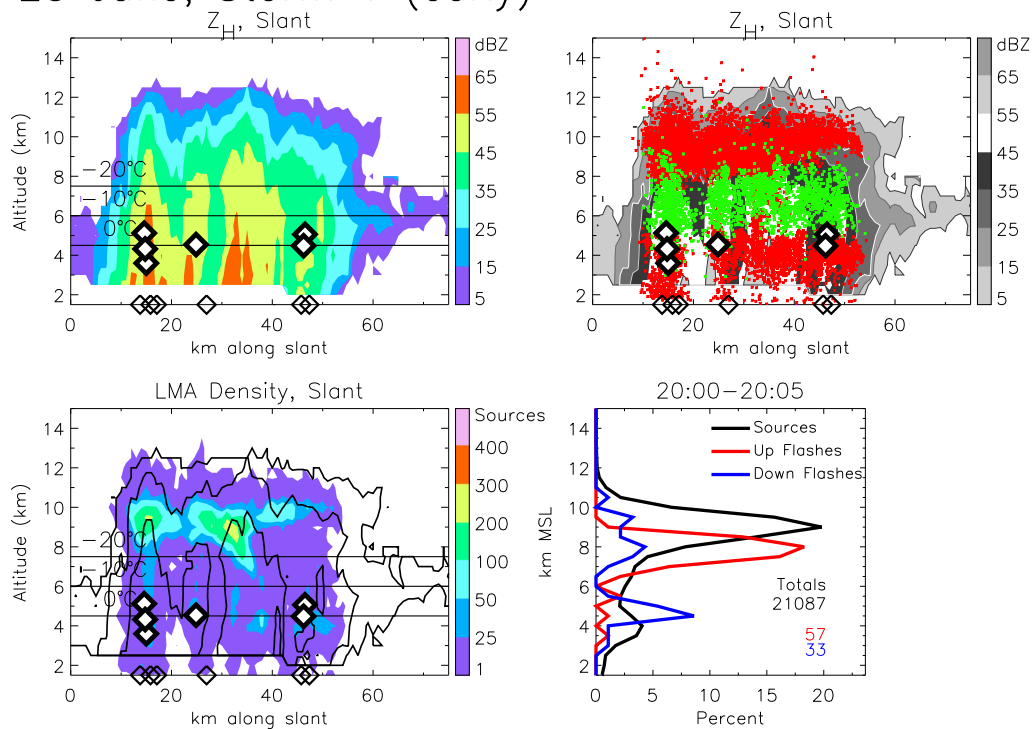


Figure 7: Representative vertical cross-sections and LMA histograms for the early -CG-dominated stage of storms observed on 23 June 2000 during STEPS. Clockwise from top-left: cross-section of horizontal radar reflectivity (Z_H); same cross-section of Z_H , but in gray scale with 5 minutes of LMA sources (2300-2305) overlaid and color-coded by charge; altitude histograms of LMA sources and flash start heights; cross-section of LMA source density with black Z_H contours at 5, 25, and 45 dBZ. The diamond symbols mark origin and strike locations of -CG flashes. Adapted from Wiens (2005).

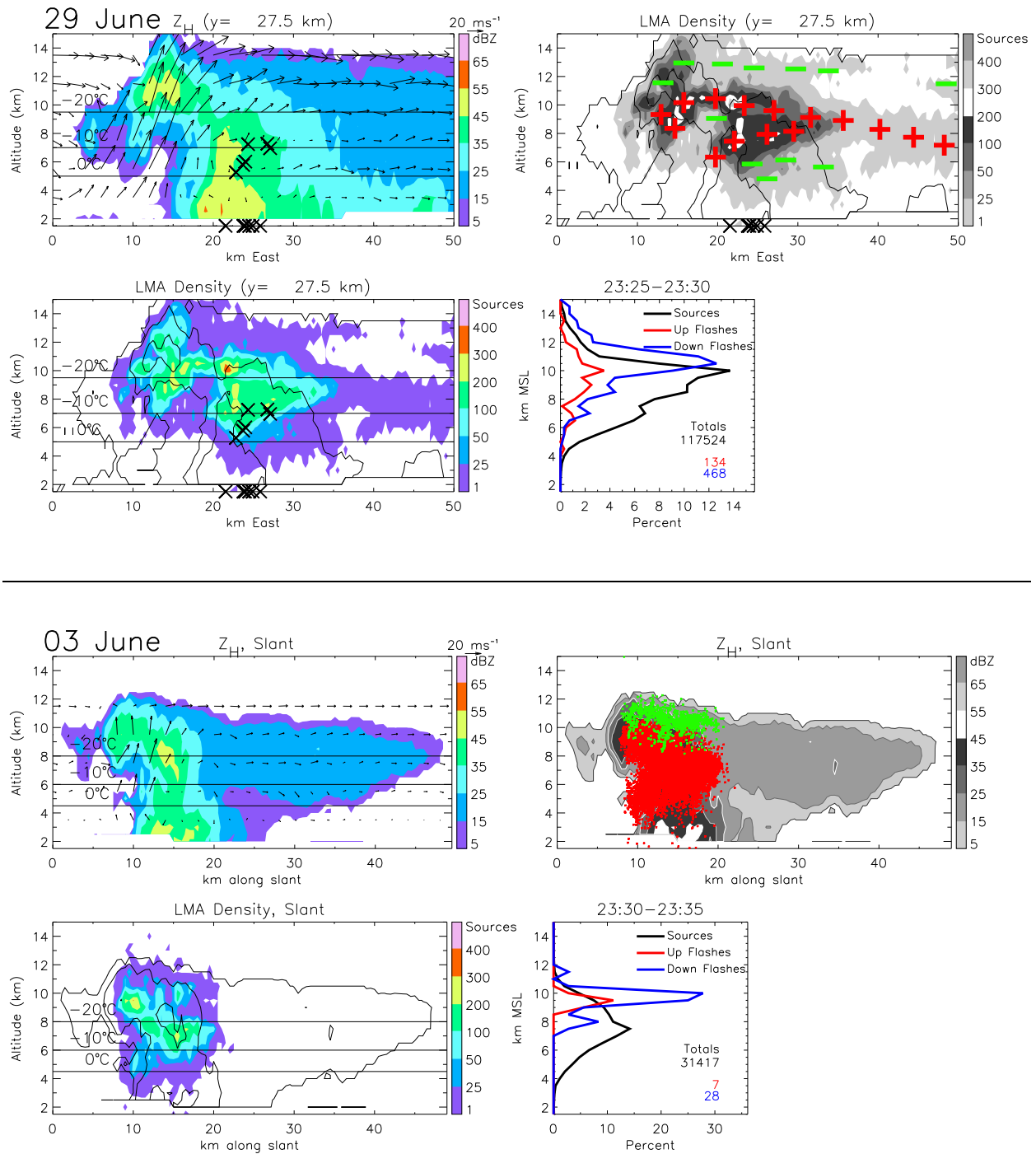


Figure 8: Representative cross-sections and LMA histograms for the storms observed on 3 and 29 June 2000 during STEPS. Layout is the same as in Fig. 7, with the addition of multi-Doppler inferred wind flow. Due to file size constraints, the top-right panel for the 29 June storm shows a composite of the LMA-inferred charge structure instead of all the individual LMA sources. The X symbols mark origin and strike locations of +CG flashes. Adapted from Wiens (2005).

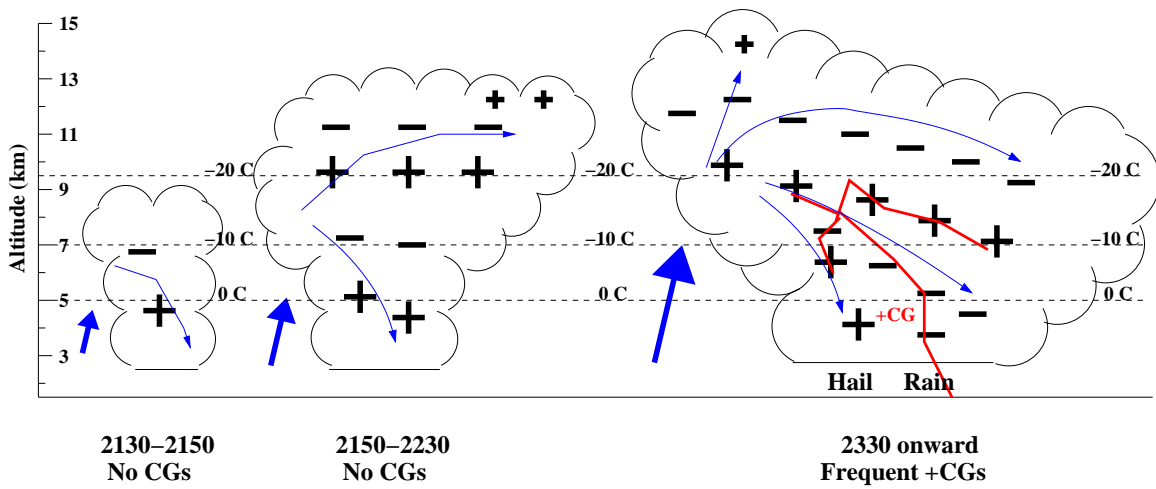


Figure 9: Schematic of the evolution of the 29 June supercell observed during STEPS. Thick blue arrows show main updraft, and thin blue arrows show air flow. The red disjointed lines indicate a +CG discharge. Adapted from Wiens et al. (2006).

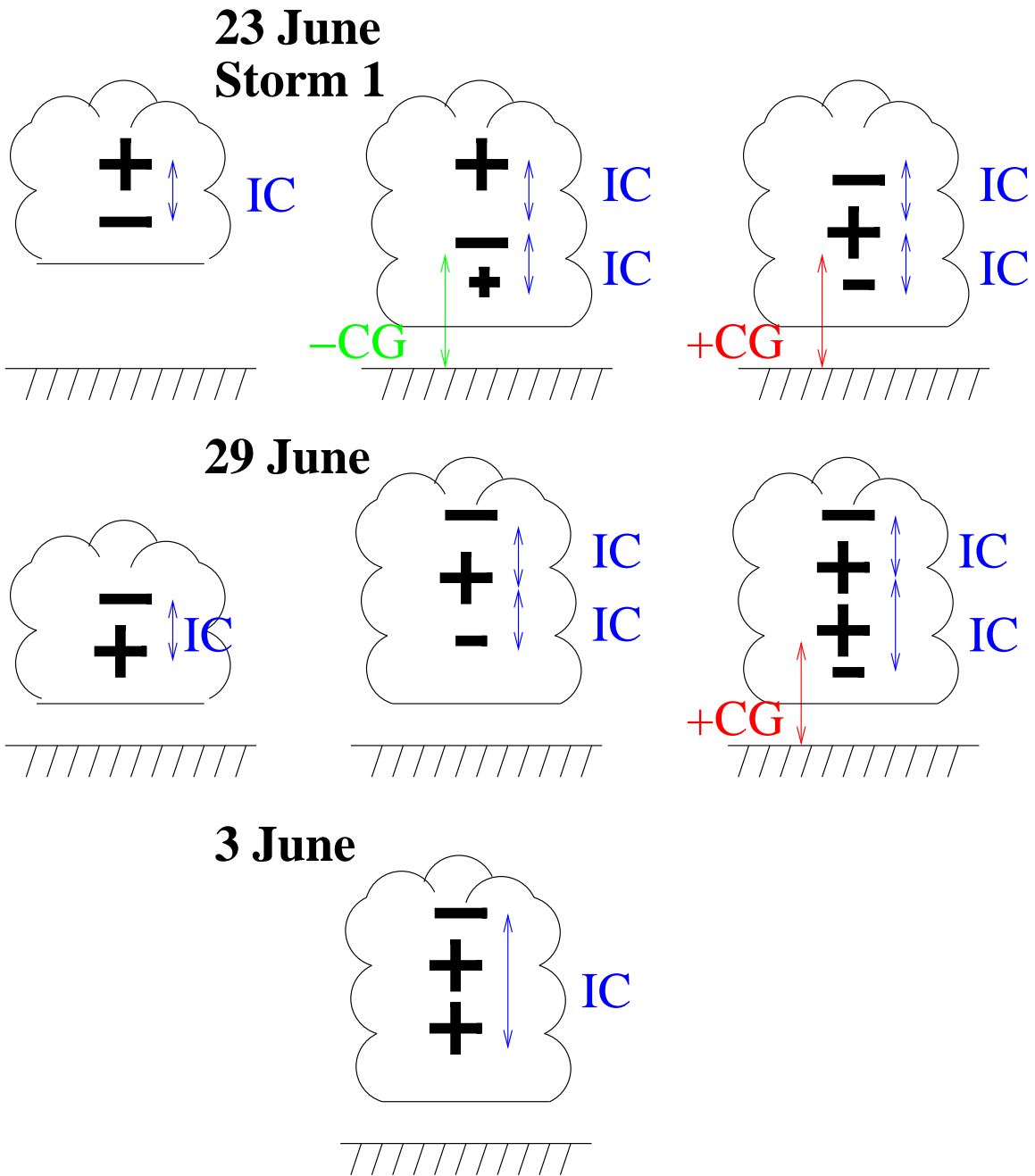


Figure 10: Simplified conceptual diagrams of the evolution of charge structure and lightning for the 23, 29, and 3 June 2000 storms observed during STEPS. Adapted from Wiens (2005).